Developmental Cognitive Neuroscience 52 (2021) 101042

Contents lists available at ScienceDirect

Developmental Cognitive Neuroscience

journal homepage: www.elsevier.com/locate/dcn

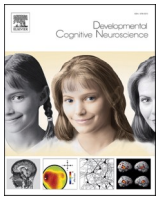

Characterizing reward system neural trajectories from adolescence to young adulthood

Zhipeng Cao [a,*], Jonatan Ottino-Gonzalez [a], Renata B. Cupertino [a], Anthony Juliano [a], Bader Chaarani [a], Tobias Banaschewski [b], Arun L.W. Bokde [c], Erin Burke Quinlan [d], Sylvane Desrivières [d], Herta Flor [e,f], Antoine Grigis [g], Penny Gowland [h], Andreas Heinz [i], Rüdiger Brühl [j], Jean-Luc Martinot [k], Marie-Laure Paillère Martinot [k,l], Eric Artiges [k,m], Frauke Nees [b,e,n], Dimitri Papadopoulos Orfanos [g], Tomáš Paus [o,v], Luise Poustka [p], Sarah Hohmann [b], Sabina Millenet [b], Juliane H. Fröhner [q], Lauren Robinson [r], Michael N. Smolka [q], Henrik Walter [i], Jeanne Winterer [i,s], Gunter Schumann [d,t,w], Robert Whelan [u], Scott Mackey [a], Hugh Garavan [a], IMAGEN consortiu

[a] Department of Psychiatry, University of Vermont College of Medicine, Burlington, VT 05401, USA
[b] Department of Child and Adolescent Psychiatry and Psychotherapy, Central Institute of Mental Health, Medical Faculty Mannheim, Heidelberg University, Square J5, Mannheim 68159, Germany
[c] Discipline of Psychiatry, School of Medicine and Trinity College Institute of Neuroscience, Trinity College Dublin, Dublin D2, Ireland
[d] Centre for Population Neuroscience and Precision Medicine (PONS), Institute of Psychiatry, Psychology & Neuroscience, SGDP Centre, King's College London, London SE5 8AF, United Kingdom
[e] Institute of Cognitive and Clinical Neuroscience, Central Institute of Mental Health, Medical Faculty Mannheim, Heidelberg University, Square J5, Mannheim 68159, Germany
[f] Department of Psychology, School of Social Sciences, University of Mannheim, Mannheim 68131, Germany
[g] NeuroSpin, CEA, Université Paris-Saclay, F-91191 Gif-sur-Yvette, France
[h] Sir Peter Mansfield Imaging Centre School of Physics and Astronomy, University of Nottingham, University Park, Nottingham NG7 2RD, United Kingdom
[i] Department of Psychiatry and Psychotherapy CCM, Charité – Universitätsmedizin Berlin, corporate member of Freie Universität Berlin, Humboldt-Universität zu Berlin, and Berlin Institute of Health, Berlin 10117, Germany
[j] Physikalisch-Technische Bundesanstalt (PTB), Braunschweig and Berlin, D-10587, Germany
[k] Institut National de la Santé et de la Recherche Médicale, INSERM U A10 "Trajectoires développementales en psychiatrie"; Université Paris-Saclay, Ecole Normale supérieure Paris-Saclay, CNRS, Centre Borelli, Gif-sur-Yvette 91191, France
[l] AP-HP. Sorbonne Université, Department of Child and Adolescent Psychiatry, Pitié-Salpêtrière Hospital, 75013, Paris
[m] Psychiatry Department, EPS Barthélémy Durand, 91152 Etampes, France
[n] Institute of Medical Psychology and Medical Sociology, University Medical Center Schleswig Holstein, Kiel University, Kiel 24118, Germany
[o] Departments of Psychiatry and Neuroscience and Centre Hospitalier Universitaire Sainte Justine, University of Montreal, Montreal, Quebec H3T 1C5, Canada
[p] Department of Child and Adolescent Psychiatry and Psychotherapy, University Medical Centre Göttingen, von-Siebold-Str. 5, Göttingen 37075, Germany
[q] Department of Psychiatry and Neuroimaging Center, Technische Universität Dresden, Dresden 01062, Germany
[r] Department of Psychological Medicine, Section for Eating Disorders, Institute of Psychiatry, Psychology and Neuroscience, King's College London, London SE5 8AF, United Kingdom
[s] Department of Education and Psychology, Freie Universität Berlin, Berlin 14195, Germany
[t] PONS Research Group, Dept of Psychiatry and Psychotherapy, Campus Charite Mitte, Humboldt University, Berlin D-10099 and Leibniz Institute for Neurobiology, Magdeburg 39118, Germany
[u] School of Psychology and Global Brain Health Institute, Trinity College Dublin, Dublin D2, Ireland
[v] Departments of Psychology and Psychiatry, University of Toronto, Toronto, Ontario M6A 2E1, Canada
[w] Institute for Science and Technology of Brain-inspired Intelligence (ISTBI), Fudan University, Shanghai 200433, PR China

ARTICLE INFO

Keywords:
Reward system
Adolescence

ABSTRACT

Mixed findings exist in studies comparing brain responses to reward in adolescents and adults. Here we examined the trajectories of brain response, functional connectivity and task-modulated network properties during reward processing with a large-sample longitudinal design. Participants from the IMAGEN study performed a Monetary

* Correspondence to: Department of Psychiatry, University of Vermont College of Medicine, Burlington 05401, VT, USA.
E-mail address: zhipeng30@foxmail.com (Z. Cao).

https://doi.org/10.1016/j.dcn.2021.101042
Received 18 July 2021; Received in revised form 5 November 2021; Accepted 1 December 2021
Available online 2 December 2021

Task-modulated network
Neural development
Monetary Incentive Delay task

Incentive Delay task during fMRI at timepoint 1 (T1; n = 1304, mean age=14.44 years old) and timepoint 2 (T2; n = 1241, mean age=19.09 years). The Alcohol Use Disorders Identification Test (AUDIT) was administrated at both T1 and T2 to assess a participant's alcohol use during the past year. Voxel-wise linear mixed effect models were used to compare whole brain response as well as functional connectivity of the ventral striatum (VS) during reward anticipation (large reward vs no-reward cue) between T1 and T2. In addition, task-modulated networks were constructed using generalized psychophysiological interaction analysis and summarized with graph theory metrics. To explore alcohol use in relation to development, participants with no/low alcohol use at T1 but increased alcohol use to hazardous use level at T2 (i.e., participants with AUDIT$\leq$2 at T1 and $\geq$8 at T2) were compared against those with consistently low scores (i.e., participants with AUDIT$\leq$2 at T1 and $\leq$7 at T2). Across the whole sample, lower brain response during reward anticipation was observed at T2 compared with T1 in bilateral caudate nucleus, VS, thalamus, midbrain, dorsal anterior cingulate as well as left precentral and postcentral gyrus. Conversely, greater response was observed bilaterally in the inferior and middle frontal gyrus and right precentral and postcentral gyrus at T2 (vs. T1). Increased functional connectivity with VS was found in frontal, temporal, parietal and occipital regions at T2. Graph theory metrics of the task-modulated network showed higher inter-regional connectivity and topological efficiency at T2. Interactive effects between time (T1 vs. T2) and alcohol use group (low vs. high) on the functional connectivity were observed between left middle temporal gyrus and right VS and the characteristic shortest path length of the task-modulated networks. Collectively, these results demonstrate the utility of the MID task as a probe of typical brain response and network properties during development and of differences in these features related to adolescent drinking, a reward-related behaviour associated with heightened risk for future negative health outcomes.

1. Introduction

Substantial effort has been expended on characterizing neurodevelopmental changes in the reward system from adolescence to adulthood (Richards et al., 2013). However, mixed findings exist in studies comparing brain responses to reward in adolescents and adults. Some studies have shown lower brain response during reward processing in adolescents relative to adults, supporting the hypothesis that heightened reward-seeking behaviors during adolescence compensate for a hypo-responsive reward system (Bjork et al., 2004; Bjork et al., 2010; Vaidya et al., 2013), while others have observed higher brain response during reward anticipation and receipt relative to adults (Ernst et al., 2005; Galvan et al., 2006; Lorenz et al., 2014). The latter pattern is often conceptualized in developmental imbalance models as suggesting that differential development of the motivational system and cognitive control system could explain heightened risk-taking behaviors during adolescence (Casey, 2015; Shulman et al., 2016; Mackey et al., 2017). Low sample size, variations in the task used to probe reward-related brain response, and cross-sectional designs may contribute to the mixed findings, which underscores the importance of a large-sample longitudinal study with a standardized task to examine reward system neural trajectories.

The monetary incentive delay (MID) task separates reward processing into discrete stages and has been widely used to probe the neural substrates of reward processing in previous fMRI studies (Oldham et al., 2018). In a previous study with a large sample of 14 year olds (N = 1510), we showed that bilateral ventral striatum (VS), caudate, pallidum, insula, thalamus, hippocampus, cingulate cortex, midbrain, motor and occipital areas show reliably fMRI response during anticipation of a large reward in contrast with no reward (Cao et al., 2019). A psychophysiological interaction analysis (PPI) also revealed widespread functional coupling between VS and cortical and subcortical regions during reward anticipation in adolescents (Cao et al., 2019). However, it is unknown how the neural correlates underlying reward anticipation in this same sample might change between 14 years old and young adulthood five years later at age 19.

Previous studies on the adolescent reward system emphasized the brain response in isolated regions such as the ventral striatum (VS) (Bjork et al., 2010; Lorenz et al., 2014). In a step towards a larger-scale understanding of the reward system, a seed-based functional connectivity analysis can examine if correlated activity between a seed region and the rest of the brain varies as a function of an experimental manipulation and varies with ageing. The functional coupling of brain responses between areas suggests their involvement in the same underlying functional processes (Lv et al., 2018). Studies have shown that functional connectivity can be found with a region that does not show a significant increase in task-related activity (Cao et al., 2019; Di and Biswal, 2019), indicating that a broader involvement of brain regions can be uncovered by a functional connectivity analysis. For instance, we have previously reported connectivity between bilateral VS and regions that play a role in attention to and integration of salient information (e.g., middle, inferior frontal gyrus, angular gyrus, inferior parietal gyrus, insula and putamen) during reward anticipation in adolescents (Cao et al., 2019). Thus, an examination of VS connectivity can probe the involvement of the non-hedonic components that are linked to the VS activity such as mobilization of attentional or cognitive resources.

Seed-based functional connectivity analysis are, however, restricted to a limited number of seed regions that are chosen by researchers (Stevens, 2016; Cao et al., 2019). As brain function is better characterized as an integrated network (Lv et al., 2018), several graph theory-based metrics (e.g., the network strength, shortest path length, clustering coefficient, efficiency) can be used to assess brain network properties in terms of topographical organization and interregional connectivity. Brain intrinsic functional connectivity undergoes dramatic changes during maturation, with increased integration and segregation facilitating network efficiency (Fair et al., 2007). In line with this finding, adults showed a more flexible and specialized intrinsic functional network compared to adolescents and children (Ernst et al., 2015). Even though the dynamics of functional connectivity can be investigated using resting-state fMRI, the task-modulated functional network, in which high-level task demands are accommodated by context-specific modulations, may offer more insights over the intrinsic functional network (Mennes et al., 2013; Di and Biswal, 2019; Finn, 2021). Therefore, an examination of task-modulated functional network properties can provide insights into the brain's functional integration and topographical organization under the task demand such as reward anticipation. However, no study has yet applied this type of network analysis in the MID task to characterize the development of the reward system.

Here, participants from a large-scale longitudinal fMRI study (IMAGEN) performed the MID task during fMRI at timepoint 1 (T1; n = 1304, mean age=14.44 years old) and timepoint 2 (T2; n = 1241, mean age=19.09 years). Brain response and functional connectivity with the VS during reward anticipation between T1 and T2 were compared using voxel-wise linear mixed-effects (LME) models. Task-modulated networks among 166 predefined regions were constructed using a generalized PPI approach for each participant (Di and Biswal, 2019), and network properties were compared between T1 and T2. According to

developmental imbalance theories and previous empirical findings (Ernst et al., 2005; Galvan et al., 2006; Lorenz et al., 2014; Casey, 2015; Shulman et al., 2016), we expected decreased brain response in reward-relevant regions such as ventral striatum, caudate, and thalamus but increased response in frontal regions during reward anticipation at T2 when compared to T1. In addition, based on previous task-fMRI and resting-state network studies (Ernst et al., 2015; Stevens, 2016), we hypothesized that functional connectivity with the VS during reward anticipation would increase and the task-modulated network would show increased network strength and decreased characteristic shortest path length at T2 when compared to T1.

To explore whether clinically problematic reward related behaviours have observable effects on developmental trajectories, we examined the impact of alcohol exposure on the neural development of reward system from adolescence to adulthood. Specifically, exploratory analyses were performed to examine the interaction between relatively high alcohol use and the trajectories of the reward system, in which brain response, functional connectivity with the VS, and graph theory metrics of the task-modulated network were compared between participants with no/low alcohol use at T1 but increased alcohol use to hazardous use level at T2 and those with consistently low alcohol use. We anticipated that relatively high alcohol use during this developmental period would interfere with the development of the reward system's brain response and task-modulated network metrics.

2. Materials and methods

2.1. Participants

The IMAGEN project collected neuroimaging data at eight sites (France, United Kingdom, Ireland, Germany) at age T1 and T2. The participants underwent the procedures described below at T1 and T2. After the quality check on neuroimaging and behavioral data, there were 1304 participants (female: 681; mean and standard deviation age: 14.44 ± 0.41 years; modal Pubertal Development Scale pubertal development status: female = 4-advaned pubertal, male=3-midpubertal) at T1 and 1241 participants (female: 639, mean and standard deviation age: 19.09 ± 0.76 years) at T2 included in the study. There were 787 participants in both T1 and T2. The project was approved by all local ethics research committees, and informed assent/consent was obtained from participants and their parents/guardians. A detailed description of the study protocol and data acquisition has been previously published (Schumann et al., 2010).

2.2. Experimental design

Participants performed a variant of the MID task (see Fig. 1). A detailed description of the MID task can be found in the Supplementary Information. Participants were familiarized with the task by performing a practice session block outside the scanner. At T1, there were 66 trials in total and 22 trials per condition. Participants were given an M&M for every 5 points they won. At T2, there were 42 trials in total and 14 trials per condition. Participants were instructed that they could exchange their points for money at the end to increase their motivation. Every participant, independently of their performance, received £/€5 (cash or vouchers). At both time points, participants were asked to win as many points as possible. The instructions given to participants at T1 and T2 are provided in the Supplementary Information. In the present study, participants who had more than 1/3 too early response trials, or 1/3 no response trials, or 50% too late response trials among all trials, or more than 50% no response or too early trials per condition were excluded from the analysis. The histograms of trial number and response time (RT) before and after applying the exclusion criteria are shown in the Supplementary Information.

2.3. Puberty development

The pubertal status of adolescents was assessed using the computerized Pubertal Development Scale (PDS) (Petersen et al., 1988), which is an 8-item self-report assessment of physical development. Pubertal status was estimated on a 5 point-scale where 1 = prepubertal, 2 = beginning pubertal, 3 = midpubertal, 4 = advanced pubertal, 5 = postpubertal. Psytools (Delosis, London), an online platform for self-assessment, was used to collect the pubertal measure.

2.4. AUDIT

The Alcohol Use Disorders Identification Test (AUDIT) is a 10-item alcohol screening questionnaire assessing alcohol consumption, alcohol-related problems and alcohol use behavior and quantifying risk from low-level to hazardous drinking (Reinert and Allen, 2002). Individual responses are scored from 0 to 4, with a maximum of 40 for the total AUDIT score. The AUDIT was assessed via online computer platforms at both T1 and T2.

2.5. MRI data acquisition

Magnetic resonance imaging (MRI) acquisition was performed with

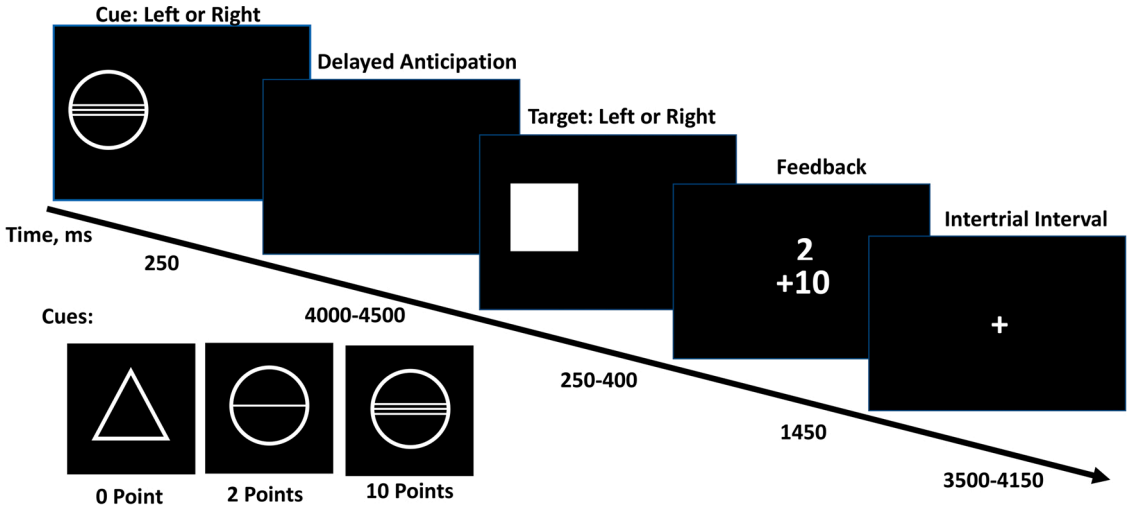

Fig. 1. Stimuli in the Monetary Incentive Delay (MID) task. Cues signaling the task condition (no reward, small reward, large reward) were displayed for 4000–4500 ms. The response and feedback phase lasted a total of 2 s. Trials were separated by a 3500–4150 ms intertrial interval.

3 T MRI systems from various manufacturers (Siemens, Philips, General Electric, and Bruker). Standardized hardware for visual and auditory stimulus presentation (Nordic Neurolabs, Bergen Norway) was used at all sites. To minimize the effects of different scanners, a set of acquisition parameters compatible with all scanners was used across sites. Full details of the MRI acquisition protocols and quality checks have been described previously (Schumann et al., 2010). The effect of MRI site was also controlled by adding it as a nuisance covariate in all statistical analyses.

2.6. fMRI data processing

2.6.1. Preprocessing

Analyses were performed using Statistical Parametric Mapping software package SPM12 (Wellcome Trust Centre for Neuroimaging, London). Time-series data were first corrected for slice-timing, then corrected for movement, non-linearly warped onto MNI space using a custom EPI template, and Gaussian-smoothed at 5 mm-full width half maximum.

2.6.2. Brain response and VS connectivity

Eight conditions were included in the individual level general linear model (GLM), which used SPM's default hemodynamic response function (HRF). The conditions were: (i) the no-reward cue, (ii) the small-reward cue, (iii) the large-reward cue, (iv) no reward (i.e., no-reward hit and miss), (v) small-reward hit, (vi) small-reward miss, (vii) large-reward hit and (viii) large-reward miss. The estimated movement was added to the individual level GLM as nuisance regressors in the form of 21 additional columns (3 translations, 3 rotations, 3 translations shifted 1 TR before, and 3 translations shifted 1 TR later) plus 9 additional regressors corresponding to the movement-related effects estimated by CompCor (Behzadi et al., 2007). In the present study, we focused on brain response during reward anticipation by contrasting the large-reward cue and the no-reward cue. Previous studies have revealed the impact of reward magnitude on reward-related responses, with larger reward eliciting greater response in reward-related regions (Bjork, et al., 2010; Yacubian, et al., 2006). Thus, we focused on the large reward trials to attain maximal sensitivity to detect associations with reward-related neural responses (Cao, et al., 2019; Schneider, et al., 2012a; Schneider, et al., 2012b). As a supplementary analysis, probabilistic maps were created to quantify robustly activated regions during reward anticipation for T1 and T2 separately (Cao, et al., 2019). Bilateral VS seed regions were chosen for reward anticipation. Connectivity maps of bilateral VS during reward anticipation were obtained using PPI analyses (Friston et al., 1997). The description of the PPI analyses can be found in the previous study (Cao et al., 2019). Head motion was calculated using mean framewise displacement (FD) (Power et al., 2012), which was included as a covariate in the subsequent statistical analysis of brain data.

Compared to the proceeding study that examined the brain response and seed-based functional connectivity during different stages of the MID task (Cao et al., 2019), the current study focused on reward anticipation but additionally examined graph theory metrics of the task-modulated network. Apart from that, there were several improvements in the current study. The previous study used 6 regressors (3 translations 3 rotations) in the individual level models. The current study included 21 movement-related regressors to better account for head motion at the individual level. Furthermore, the mean FD was calculated and included in the group level models to address head motion at the group level analyses in the present study. In addition to the image quality, the current study additionally excluded participants who did not meet the behavioral inclusion criteria and those who failed in task-modulated network construction, which resulted in a smaller number of participants at T1 when compared to that of the previous paper.

2.6.3. Task-modulated network

A functional connectivity network that was modulated by reward anticipation (large-reward cue minus the no-reward cue) was built using a generalized PPI approach among multiple brain regions of interest (ROIs) (Di and Biswal, 2019). The ROIs were selected based on a functionally pre-defined atlas (Dosenbach-160) that consists of 160 regions with both good spatial coverage and resolution (Dosenbach et al., 2010). Spherical ROIs with a 5-mm radius centered at MNI coordinates obtained from Dosenbach-160 were created. Six additional ROIs (bilateral ventral striatum: [−12,14,−8], [12,14,−8]; bilateral amygdala: [20,−4,−15], [−20,−6,−15]; bilateral parahippocampus: [−20,−33,−4], [14,−33,−7]) were added as they are structures associated with reward processing but not included in the atlas.

For a certain $ROI_{(i)}$, the first eigenvariate of the time course was extracted, and variance in the eigenvariate attributable to the head motion was removed. The extracted eigenvariate was deconvolved from the HRF and then multiplied with the two psychological variables of interest (i.e., the large-reward cue and the no-reward cue). The two resulting PPI terms were convolved with the HRF to obtain the BOLD-level PPI variables. Finally, the extracted eigenvariate of $ROI_{(i)}$, the BOLD PPI variables (the large-reward cue and the no-reward cue), the psychological variables (the large-reward cue and the no-reward cue) and one constant term, that is 6 regressors in total, were regressed against the extracted eigenvariate from another $ROI_{(j)}$ using the GLM. The functional connectivity between $ROI_{(i)}$ and $ROI_{(j)}$ that was modulated by the experimental context (i.e., large-reward minus no-reward cue) was obtained by contrasting the resulting beta weights that corresponded to the BOLD PPI effects. When repeated over all pairs of ROIs, the result was an ROI-by-ROI matrix whose elements were task-modulated functional connectivity. As a pair of ROIs had two estimates of functional connectivity, the resulting connectivity matrix was averaged along the diagonal to get mean functional connectivity between pairs of ROIs (Di and Biswal, 2019).

2.7. Statistical analysis

The analytical strategies and the numbers of participants included in each analysis are illustrated in Fig. 2. There were 1491 participants at T1 and 1365 participants at T2 who passed image quality control (QC) and 1304 and 1241 participants who further passed behavioural QC and the latter groups were included in the analysis examining the trajectories of brain response, functional connectivity of the VS, and graph theory metrics of the task-modulated network. The number of years between two visits was imputed for participants missing this variable (this was a nuisance covariate of no interest with a tight distribution around five years given the study design). There were 674 participants who met the inclusion criteria based on the completeness and cutoffs of the AUDIT, which entered the second set of analyses assessing the interactive effects between alcohol use and trajectories of the brain measures.

2.7.1. Behavioral performance

Response times (RT) for each condition were compared between T1 and T2 using the LME model in which a participant's sex, recruitment site, handedness, PDS at baseline (mode centered), sampling time (T1 or T2, with T1 as reference) and age differences between T1 and T2 were included as fixed effects. Participant ID was included as a random effect. The age differences between T1 and T2 were included in the LME model to capture the difference in sampling intervals between participants. For participants who were only sampled at one time point, the mean sampling interval (4.59 years) was used as the age difference. The significance of the sampling time effects was assessed using a permutation test in which null models were built by randomly shuffling the time label (i.e., T1 and T2) 1000 times. For participants who presented at both T1 and T2, their time labels were randomly shuffled within participants. For participants who only presented at T1 or T2, their time labels were randomly shuffled as a group to maintain the same number of

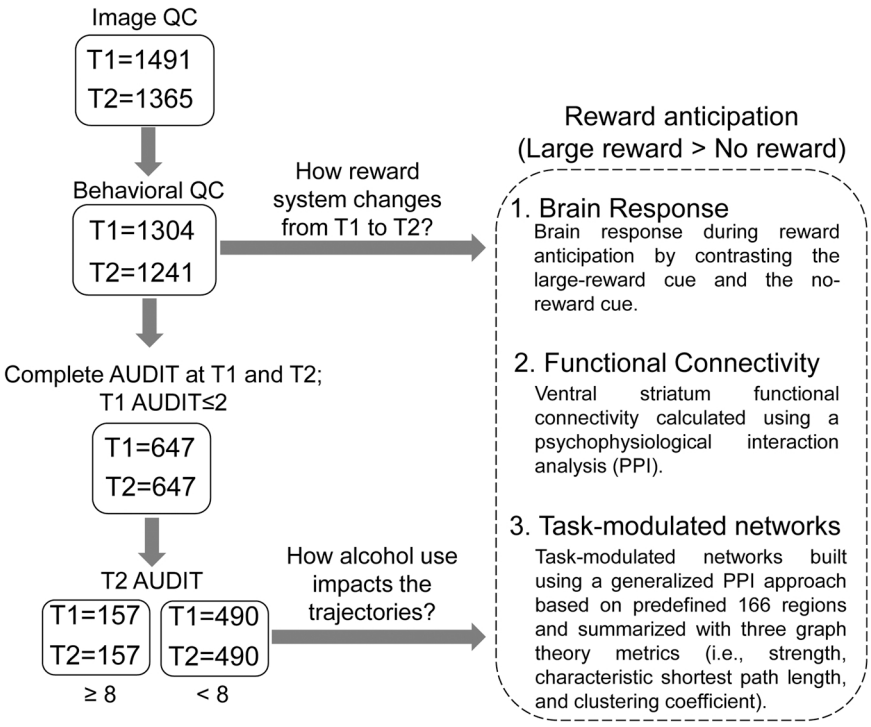

Fig. 2. Analytical strategies on brain measures. There were 1491 participants at T1 and 1365 participants at T2 who passed image quality control (QC) and 1304 and 1241 participants who further passed behavioural QC. These participants were included in the analyses examining the trajectories of brain response, functional connectivity of the ventral striatum, and graph theory metrics of the task-modulated network. 674 participants met the inclusion criteria based on the completeness and cutoffs of the Alcohol Use Disorders Identification Test (AUDIT) and were included in the second set of analyses assessing the interactive effects between alcohol use and trajectories of the brain measures.

participants at T1 and T2 in the null model. The 95th percentiles (i.e., bottom 2.5% and upper 97.5%) of the resulting null distribution were used as the threshold. As the results of brain response showed significant differences in left and right motor areas, the ratio of the responses made by the left vs. right hand was calculated and compared between T1 and T2.

2.7.2. Brain response and VS connectivity

We first compared brain response during reward anticipation between T1 and T2 data with voxel-wise linear mixed-effects (LME) models as described in the previous section. Mean FD was additionally included in the LME model as a fixed effect to mitigate the influences of head motion. Threshold-free cluster enhancement (H = 2, E = 0.5, C = 18, dh = 0.1) was separately applied to the positive and negative t-value maps to identify contiguous areas of differences (Smith and Nichols, 2009). A permutation test and a voxel-wise FWE correction were used to determine the significance of the TFCE values separately for positive and negative t-value maps. For each iteration of the permutation test, a set of null voxel-wise TFCE values were obtained by randomly shuffling the time label (i.e., T1 or T2) using the same strategy described above and then the maximum TFCE value was derived. The process was repeated 1000 times and the value corresponding to the 95th percentile of the derived maximum TFCE values was used as the FWE-corrected threshold.

When reporting the results, the peak TFCE value, corresponding MNI coordinates and the number of suprathreshold voxels within a customized AAL atlas that included ventral striatum and midbrain ROIs were reported. The same voxel-wise analytical strategy was adopted to compare functional connectivity with left or right VS during reward anticipation between T1 and T2. The effect size of sampling time was calculated as

$$\text{Cohen's} \quad d = \frac{t \times (n1 + n2)}{\sqrt{(n1 \times n2)} \times \sqrt{df}}$$

where n1 and n2 represent the numbers of participants at T1 and T2, respectively, and df is degrees of freedom. To examine brain regions that were robustly activated during reward anticipation in the MID task, probabilistic maps were created and shown in the Supplementary Information.

2.7.3. Network analysis

For task-modulated functional networks at the individual level, sparsity thresholds from 5% to 40% with increments of 2% were used to define supra-threshold connections and then global network measures (i.e., strength, characteristic shortest path length, and clustering coefficient) were calculated to characterize the global network properties of the task-modulated network. Network connectivity strength characterizes the sum of weights of supra-threshold links among nodes. The shortest path is a path with the minimum sum of edges between a pair of nodes. The characteristic shortest path length is the average number of shortest path lengths for all possible pairs of nodes in the network and it reflects how efficiently the network exchanges information. A node clustering coefficient is calculated as the number of closed triangles divided by the number of all possible closed triangles around the node. The network clustering coefficient is the average of the clustering coefficients of all the nodes, which measures the extent to which the nodes in the network tend to cluster together. Detailed formulas and calculation for these graph theory metrics can be found in previous studies (Wang et al., 2011; Wang et al., 2015).

As noted above, to ensure the graph-theory based metrics were independent of the selection of the threshold, a range of sparsity thresholds (i.e., 5–40%) was used to define supra-threshold connections. The area under the curve (AUC) that aggregated the metric over the sparsity thresholds was calculated as a sparsity independent measure and was then compared between T1 and T2 using the same analytical strategy adopted in the behavioral performance analysis, with mean FD additionally included as a fixed effect in the LME models.

2.7.4. Alcohol use effects

The relationship between alcohol use and neural development of the reward system was explored. Only participants who completed the AUDIT at both T1 and T2 and reported no/low problematic drinking (i.e., AUDIT $\leq$ 2) at T1 were included (n = 647). A previous study showed that a cutoff of AUDIT $\geq$ 3 offered a good balance of sensitivity and

specificity in detecting any alcohol use problems (sensitivity: 0.72; specificity: 0.89) as well as alcohol abuse or dependence (sensitivity: 0.88; specificity: 0.77) among adolescents (14–18 years) (Knight et al., 2003). Participants who reported an AUDIT total score ≥ 3 at T1 were excluded because they may have already experienced brain changes correlated with alcohol use. At T2 when alcohol use is more normative (the median AUDIT score was 6), participants who had an AUDIT total score ≤ 7 were designated as low-risk alcohol users and those who had an AUDIT total score ≥ 8 were considered as problematic drinkers. The cutoff used for T2 (≥8) is recommended for AUDIT in detecting problematic alcohol use in adults (Conigrave et al., 1995; WHO, 2001), which has shown relatively high sensitivity (0.82) and specificity (0.78–0.79) among young adults (18–25 years) (O'Connor et al., 2018). We defined those who had a low AUDIT score (≤2) at T1 but a high AUDIT score (≥8) at T2 as the high alcohol use group (HA). Those who had a low AUDIT score at both T1 (≤2) and T2 (≤7) were designated the low alcohol use group (LA). We performed four sensitivity analyses to test if the observed alcohol effects with a T1 cutoff of ≥ 3 and a T2 cutoff of ≥ 8 replicate when: (1) using a different AUDIT cutoff (≥2) at T1; (2) using a variety of AUDIT cutoffs (≥6–13) at T2; (3) using top and bottom 25th percentiles for AUDIT at T2 to define HA and LA groups; (4) using changes of the AUDIT score as a continuous measure instead of defining HA and LA groups. Details can be found in the Supplementary Information. Given that our analytic design already restricted our focus to participants to participants with low AUDIT (≤2) at T1, the exclusion of participants who had dropped out of the study by T2 was unlikely to reduce the variance in AUDIT at T1. Additional analyses were performed to test this in the Supplementary Information.

To examine if the changes in reward-related functioning from T1 to T2 were different in those who engaged in relatively high alcohol use at T2 as compared to low alcohol use, we used similar LME models as described above but with the interaction terms between the time of the scan (T1 vs T2, with T1 as reference) and group (HA vs. LA, with LA as reference) included as fixed effects. The interaction effects on the brain measures including voxel-wise brain response, VS connectivity, network properties were tested against 1000 null models in which the label of the alcohol use group was randomly shuffled. For the significant interactions, pairwise comparisons of two factors of interest (i.e., time and group) were performed as post-hoc analysis. The FDR was used to as multiple comparisons correction method in the post-hoc analysis.

2.8. Software and visualization

fMRI data processing and network construction were performed using MATLAB (version 9.6.0; Natick, Massachusetts: The MathWorks Inc) and SPM12. GRENTNA was used to calculate graph-based measures (Wang et al., 2015). The longitudinal analyses were performed using R (version 3.6) and lmerTest (Kuznetsova et al., 2017). MRIcronGL was used for brain data visualization (Rorden and Brett, 2000). Open-visualization (https://github.com/jorvlan/open-visualizations) and R package "interaction" were used for data visualization. R package "emmeans" were used for post-hoc analysis. Computations were performed, in part, on the Vermont Advanced Computing Core.

3. Results

3.1. Participants

Participant characteristics at T1 and T2 are shown in Table 1. The comparisons of RT between T1 and T2 indicated lower RT for large ($t = -17.45$, 95% interval of the null distribution: [−1.60, 2.16]), small ($t = -17.26$, [−1.52, 2.34]) and no ($t = -19.64$, [−1.60, 2.19]) reward conditions at T2 compared to T1. No significant difference was observed in the ratio of responses made by left vs. right between T1 and T2 ($t = 1.27$, [−2.05, 2.11]; Fig. S5). The comparisons of RT between large and no reward condition indicated participants responded faster to large reward than no reward at both T1 ($t = -21.54$, [−1.77,2.00]) and T2 ($t = -15.46$, [−2.09,1.95]).

Table 1
Characteristics of participants at T1 and T2.

	T1 (N = 1304)	T2 (N = 1241)	*p*
Sex, n (%)			0.74
Male	623 (48)	602 (49)	
Female	681 (52)	639 (51)	
Age, years			
mean ± sd	14.44 ± 0.41	19.09 ± 0.76	
Handedness, n (%)			0.63
Left	141 (11)	126 (10)	
Right	1163 (89)	1115 (90)	
mean FD			
mean ± sd	0.25 ± 0.17	0.17 ± 0.10	< 0.05
T1 PDS*, n (%)			0.95
Pre-pubertal(1)	9 (1)	8 (1)	
Beginning pubertal(2)	73 (6)	76 (6)	
Mid-pubertal(3)	399 (31)	365 (29)	
Advanced pubertal(4)	744 (57)	719 (58)	
Post-pubertal(5)	79 (6)	73 (6)	
Left/Right response ratio			
mean ± sd	1.07 ± 0.31	1.09 ± 0.33	0.21
RT (ms), mean ± sd			
Large reward	246.35 ± 31.75	228.70 ± 32.02	
Small reward	254.84 ± 36.44	234.42 ± 34.43	
No reward	278.77 ± 45.75	249.39 ± 40.48	
Large-No reward	-32.42 ± 33.87	-20.69 ± 29.86	

FD: Framewise displacement; RT: Response time; PDS: Pubertal development stage. Two sample *t*-test was used to compare mean FD and chi-square tests were used to compare sex, handedness and baseline PDS respectively between T1 and T2. * Participants are assumed to be post-pubertal at T2. As the participants are not matched between T1 and T2, the T1 PDS is also reported for participants at T2.

3.2. Brain response

Table 2 and Fig. 3 show regions with significant changes in brain response during reward anticipation between T2 and T1. Participants showed lower brain response in bilateral caudate, VS, thalamus, midbrain, dorsal anterior cingulate cortex (dACC) and left precentral and postcentral gyrus but greater response in bilateral inferior frontal gyrus (IFG), middle frontal gyrus (MFG) and right precentral and postcentral gyrus at T2 when compared to T1. Regions showed robust responses (probability of activation ≥ 0.8) during reward anticipation at T1 and T2 are shown in the Supplementary Information.

3.3. VS connectivity

Table 3 and Fig. 4 illustrate regions with significant increases in functional connectivity with the left and right VS during reward anticipation from T1 to T2. Both left and right VS showed increased connectivity with bilateral temporal, parietal and occipital gyrus at T2 compared to T1. In addition, left VS had increased connectivity with bilateral superior frontal, inferior frontal gyrus, and median cingulate gyri. No regions showed significantly decreased functional connectivity with the VS from T1 to T2.

3.4. Network properties

As shown in Fig. 5, significant lower characteristic shortest path length ($t = -55.809$, 95% interval of null distribution: [−0.95,2.48]) and greater network strength ($t = 58.73$, [−2.61, 1.20]) were observed at T2 compared to T1. However, the difference in clustering coefficient ($t = -1.93$, [−1.94, 1.94]) did not reach statistical significance.

Table 2
Regions showing significantly increased (A) and decreased (B) brain response during reward anticipation at T2 as compared to T1. For each region, the number of significant voxels, peak TFCE values and the corresponding MNI coordinates are reported.

Regions	Voxel Number	Peak Intensity	x	y	z
A. T2 > T1					
Inferior Frontal Gyrus, Opercular Part (L)	43	827	-54	11	10
Inferior Frontal Gyrus, Orbital Part (L)	85	1032	-36	35	-8
Inferior Frontal Gyrus, Orbital Part (R)	25	515	30	35	-8
Inferior Frontal Gyrus, Triangular Part (L)	324	829	-51	29	25
Inferior Frontal Gyrus, Triangular Part (R)	64	505	54	32	13
Middle Frontal Gyrus (L)	16	643	-48	41	16
Precentral Gyrus (R)	148	2269	39	-22	55
Postcentral Gyrus (R)	223	2225	42	-22	52
Insula (R)	29	1087	39	-13	16
Rolandic Operculum (R)	97	1133	51	-16	16
Supramarginal Gyrus (R)	54	872	60	-16	22
Superior Temporal Gyrus (R)	14	835	48	-25	16
Middle Occipital Gyrus (L)	65	644	-42	-76	31
Middle Temporal Gyrus (L)	52	646	-45	-67	16
Parahippocampal Gyrus (L)	23	733	-30	-43	-8
Precuneus (L)	31	566	-9	-58	13
Lingual Gyrus (L)	11	667	-24	-46	-8
Angular Gyrus (L)	54	660	-45	-67	25
Cuneus (L)	12	522	-18	-61	19
Calcarine (L)	40	552	-12	-52	10
Fusiform Gyrus (L)	45	805	-27	-46	-11
Fusiform Gyrus (R)	10	411	27	-43	-14
Cerebellum (L)	140	787	-18	-52	-17
B. T1 > T2					
Superior Frontal Gyrus (L)	41	4385	-27	-10	73
Superior Frontal Gyrus, Medial (L)	71	1269	0	20	40
Superior Frontal Gyrus, Medial (R)	36	787	3	50	4
Anterior Cingulate Gyri (L)	96	1336	0	29	28
Anterior Cingulate Gyri (R)	138	1397	3	11	28
Supplementary Motor Area (L)	217	2484	-3	-10	49
Supplementary Motor Area (R)	172	1641	3	-4	64
Median Cingulate Gyri (L)	157	2473	-3	-7	49
Median Cingulate Gyri (R)	137	1379	3	14	31
Ventral Striatum (L)	3	420	-12	14	-8
Ventral Striatum (R)	3	751	12	14	-8
Caudate (L)	34	793	-12	-7	19
Caudate (R)	66	976	6	17	1
Midbrain (L)	82	820	-9	-25	-5
Midbrain (R)	32	648	3	-31	1
Thalamus (L)	137	1997	-12	-19	10
Thalamus (R)	111	1417	6	-22	10
Paracentral Lobule (L)	118	1890	-15	-34	64
Postcentral Gyrus (L)	397	17564	-42	-25	55
Precentral Gyrus (L)	307	17144	-39	-25	61
Precentral Gyrus (R)	18	369	21	-31	70
Precuneus (L)	93	1060	0	-37	58
Precuneus (R)	103	854	12	-73	49
Cuneus (L)	66	2668	-9	-97	16
Cuneus (R)	28	818	6	-82	16
Calcarine (L)	181	3206	-9	-88	-2
Calcarine (R)	62	1008	24	-97	1
Fusiform Gyrus (L)	82	1937	-33	-82	-17
Lingual Gyrus (L)	174	3189	-12	-88	-2
Lingual Gyrus (R)	84	1344	9	-67	-8
Superior Parietal Gyrus (L)	77	1466	-24	-40	64
Superior Parietal Gyrus (R)	44	843	12	-70	52
Inferior Parietal Gyrus (L)	21	1890	-45	-28	46
Superior Occipital Gyrus (L)	89	3230	-18	-97	16
Superior Occipital Gyrus (R)	24	986	21	-97	4
Inferior Occipital Gyrus (L)	116	1975	-36	-85	-8
Inferior Occipital Gyrus (R)	28	986	24	-94	-2
Middle Occipital Gyrus (L)	220	3340	-21	-97	13
Middle Occipital Gyrus (R)	20	1011	24	-97	4
Cerebellum (L)	794	2504	-9	-82	-17
Cerebellum (R)	1406	2445	18	-52	-23

3.5. Alcohol use effects

The characteristics of participants included in the analysis are shown in Table S2. Voxel-wise analysis revealed no significant interaction effects between alcohol use group (HA vs. LA) and time (T1 vs. T2) on brain response or functional connectivity with left VS. However, a significant positive interaction was observed for functional connectivity between right VS and left middle temporal gyrus (voxel number: 22, Peak: 343, MNI: −57 −61 −2, FWE-corrected $p < 0.05$; see Fig. 6). Post-hoc analysis was performed with functional connectivity with right VS extracted within a spherical ROI with a 5-mm radius centered at the MNI, which suggested LA had greater functional connectivity between right VS and left middle temporal gyrus than HA at T1 ($t = 2.70$, FDR-corrected $p < 0.05$) but the connectivity was lower than HA at T2 ($t = -3.10$, FDR-corrected $p < 0.05$). HA had increased connectivity between right VS and left middle temporal gyrus from T1 to T2 ($t = -5.51$, FDR-corrected $p < 0.001$), while there was no significant difference in LA between T1 and T2 ($t = -0.16$, FDR-corrected $p = 0.88$). The results of pairwise differences of time and group in the functional connectivity of left middle temporal gyrus are shown in Table S3.

For the task-modulated network, there was no significant interaction observed for network strength ($t = -0.65$, [−1.64, 1.63]) or network clustering coefficients ($t = -0.57$, 95% interval of null distribution: [−2.13, 2.27]). However, as shown in Fig. 6, the positive interaction was significant on the characteristic shortest path length ($t = 2.52$, [−1.94, 2.00]). Post-hoc analysis suggested the characteristic shortest path length in LA ($t = 37.43$, FDR-corrected $p < 0.001$) and HA ($t = 18.72$, FDR-corrected $p < 0.001$) decreased from T1 to T2. LA had lower characteristic shortest path length than HA at T2 ($t = -2.46$, FDR-corrected $p < 0.05$), while there was no significant difference between LA and HA at T1 ($t = 0.90$, FDR-corrected $p = 0.37$). The results of pairwise differences of time and group in the characteristic shortest path length are shown in Table S3.

The results of the sensitivity analyses indicated that splitting HA and LA based on the AUDIT cutoff (≥8) at T2 yielded reliable results, especially for the interactive effects of increased alcohol on the right VS connectivity with left middle temporal gyrus. The interaction effects remained significant in sensitivity analyses (1), (2) with cutoffs (≥6–10), (3) and (4). The interaction effects for the characteristic shortest path length were replicated when using a different cutoff at T1 (≥2) as well as using different cutoffs at T2 (≥7, ≥9). The interaction effects were non-significant in sensitivity analyses (3) and (4) but showed a same positive trend. It should be noted that the reduced sample size in HA group with higher T2 cutoffs in the sensitivity analysis (2) and in both HA and LA groups in the sensitivity analysis (3) can lower the statistical power to detect subtle effects. Examining brain effects at each level of the AUDIT would suffer from low statistical power. Aggregating group data according to a recommended AUDIT cutoff may provide better insights with regard to the subtle effects.

4. Discussion

In the present study, we employed neuroimaging data from a large-scale longitudinal study to examine reward system maturation from early adolescence to young adulthood. Voxel-wise LME models revealed

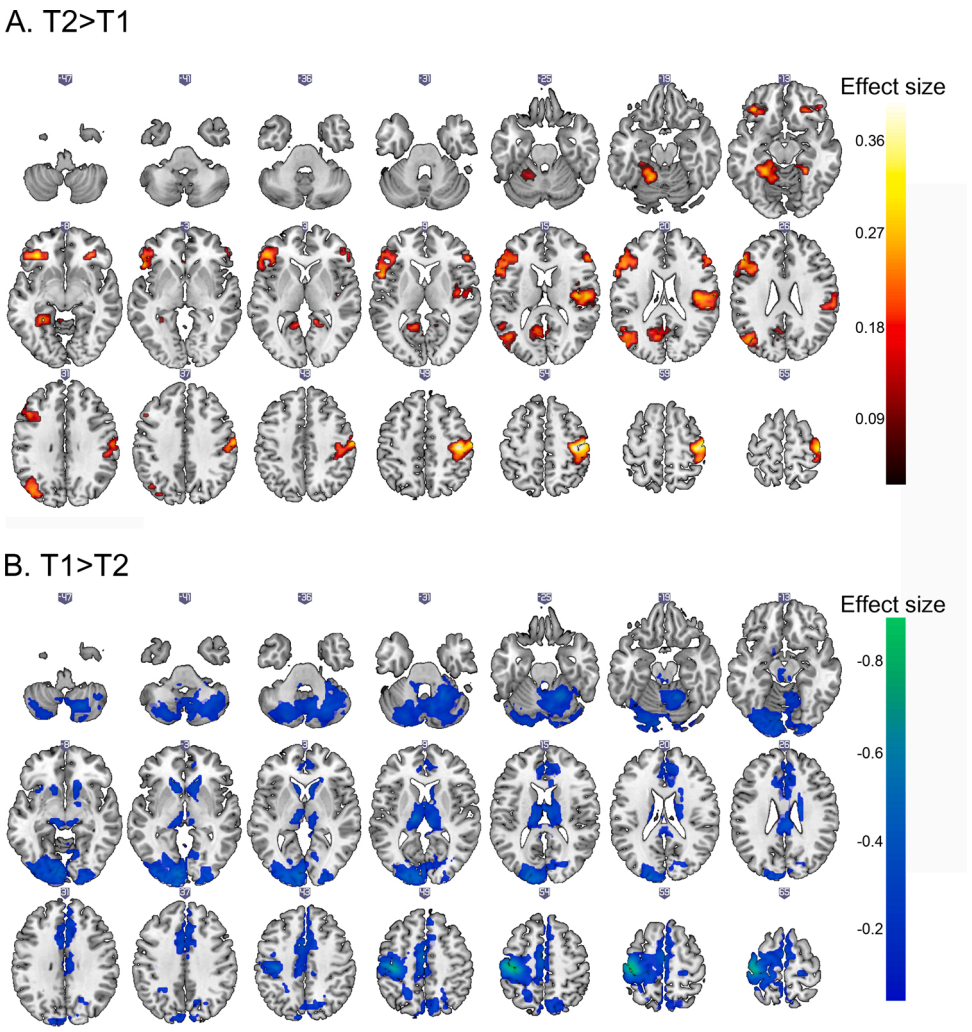

Fig. 3. Regions showing significantly increased (A) and decreased (B) brain response during reward anticipation at T2 as compared to T1. The colorbar denotes the effect size.

decreased brain response in subcortical regions such as bilateral caudate, VS, thalamus, midbrain but increased brain response in the frontal cortex (e.g., IFG, MFG) during reward anticipation at T2 compared to T1. Increased functional connectivity with VS and a more topologically efficient task-modulated functional network during reward anticipation were found. In the exploratory analysis comparing participants who engaged in relatively high alcohol use at T2 with those who did not, significant interactions between alcohol use and time (T1 vs. T2) were found in functional connectivity between right VS and left MTG as well as the characteristic shortest path length of the task-modulated network.

Decreased VS response during reward anticipation was observed at T2 compared to T1, which supports previous findings that adolescents display heightened response in VS during reward processing (Ernst et al., 2005; Galvan et al., 2006; Lorenz et al., 2014). Also, increased IFG and MFG response at T2 was observed, which is consistent with theories of neural development imbalance between the limbic and prefrontal control regions during adolescence (Casey, 2015; Shulman et al., 2016). Interestingly, at T2 compared to T1, we found significantly less response in the left precentral and postcentral gyrus but greater response in the right precentral and postcentral gyrus. The analysis of button presses (left vs. right hand) demonstrated that there was no significant difference between T1 and T2 in the ratio of left- and right-hand responses during the MID task. These results from the longitudinal analysis are consistent with the cross-sectional probabilistic mapping results in the supplementary analysis showing that the robust motor response pattern (probability of activation $\geq$ 0.8) in precentral and postcentral gyrus during reward anticipation was bilateral at T1 but unilateral at T2. A previous meta-analysis of 50 MID studies, the majority of which studied adult samples, reported activation of the right supplementary motor area and premotor area during reward anticipation (Oldham et al., 2018). It is possible that the right hemisphere specific response in the motor area is a characteristic of anticipation of large reward in contrast to no reward in adults.

A body of literature has shown that reward-related regions such as the VS can be recruited not only for reward-specific processes but also in the service of vigilance or other cognitive demands, even in the absence of reward (Sarter et al., 2006; Boehler et al., 2011; Breckel et al., 2011; Vassena et al., 2014). For instance, Boehler and colleagues reported that participants had greater VS response in a high-demand cognitive task when compared to a low-demand task, suggesting the VS is also involved in the recruitment of processing resources even in the absence of monetary reward (Boehler et al., 2011). It is possible that the VS response observed during reward anticipation may reflect a combination of response to anticipatory affect (i.e., delight at reward prospects) and mobilization of attentional or cognitive resources. Thus, decreased VS response from T1 to T2 would be consistent with the adolescent VS response stemming more from anticipatory affect while the adult response may stem more from non-hedonic processes such as mobilization of attentional or cognitive resources. In support of this idea, we

Table 3
Regions showing significantly increased functional connectivity with left (A) and right (B) VS during reward anticipation at T2 as compared to T1. For each region, the number of significant voxels, peak TFCE values and the corresponding MNI coordinates are reported.

Regions	Voxel Number	Peak Intensity	x	y	z
A. Left VS					
Middle Frontal Gyrus (R)	24	350	48	44	19
Superior Frontal Gyrus, Medial (L)	78	393	0	35	46
Inferior Frontal Gyrus, Triangular Part (L)	8	337	-48	32	28
Superior Frontal Gyrus, Medial (R)	32	370	3	32	46
Median Cingulate Gyri (L)	16	370	-3	29	34
Inferior Frontal Gyrus, Triangular Part (R)	9	323	57	29	19
Superior Frontal Gyrus (L)	30	354	-21	23	58
Superior Frontal Gyrus (R)	17	345	21	23	58
Middle Frontal Gyrus (L)	33	372	-27	8	64
Median Cingulate Gyri (R)	48	360	3	-46	37
Inferior Parietal Gyrus (R)	40	359	42	-55	49
Angular Gyrus (R)	80	364	42	-58	49
Middle Temporal Gyrus (L)	123	604	-60	-61	7
Middle Temporal Gyrus (R)	41	379	57	-61	7
Inferior Temporal Gyrus (L)	31	580	-57	-64	-8
Superior Parietal Gyrus (R)	20	349	36	-64	55
Middle Occipital Gyrus (L)	139	515	-27	-67	31
Inferior Occipital Gyrus (L)	9	434	-54	-70	-5
Precuneus (L)	86	381	0	-70	34
Precuneus (R)	90	392	6	-70	34
Cuneus (R)	22	405	6	-73	28
Superior Parietal Gyrus (L)	20	366	-27	-76	46
Cuneus (L)	45	395	0	-76	31
Middle Occipital Gyrus (R)	29	336	33	-76	31
Inferior Parietal Gyrus (L)	5	483	-30	-82	43
Superior Occipital Gyrus (L)	23	448	-24	-85	37
B. Right VS					
Inferior Temporal Gyrus (R)	6	371	57	-25	-17
Supramarginal Gyrus (R)	26	337	48	-40	28
Middle Temporal Gyrus (R)	198	439	60	-40	1
Superior Parietal Gyrus (R)	5	359	51	-43	58
Supramarginal Gyrus (L)	9	344	-57	-52	28
Inferior Parietal Gyrus (R)	81	443	54	-52	52
Inferior Temporal Gyrus (L)	16	478	-54	-67	-8
Angular Gyrus (L)	20	367	-39	-67	37
Angular Gyrus (R)	135	414	51	-67	37
Middle Temporal Gyrus (L)	98	488	-54	-70	1
Middle Occipital Gyrus (L)	93	486	-51	-73	1
Inferior Occipital Gyrus (L)	19	433	-51	-73	-5
Superior Parietal Gyrus (L)	29	431	-12	-73	52
Precuneus (L)	142	444	-6	-73	40
Cuneus (L)	16	435	0	-73	34
Precuneus (R)	66	430	6	-73	37
Inferior Parietal Gyrus (L)	25	415	-30	-82	43
Superior Occipital Gyrus (L)	14	416	-21	-82	43

found age-related increases in VS functional connectivity with fronto-parietal regions such as the inferior frontal gyrus, parietal gyrus, middle and inferior occipital gyrus which play important roles in value-driven attention capture and in controlling attentional resources (Corbetta and Shulman, 2002; Anderson, 2016).

Further analysis of functional connectivity among 166 pre-defined ROIs revealed more network connectivity strength and lower characteristic shortest path length at T2. Transformations in task-modulated network efficiency found in the present study are consistent with previous findings from resting-state studies showing more flexible and efficient brain organization in older individuals (Ernst et al., 2015). Also, increased functional connectivity with VS, network strength and efficiency are consistent with previous task-fMRI studies showing greater seed-based functional connectivity in adults compared to adolescents (Stevens, 2016). Paralleling the previous findings in resting-state studies, the current results indicate that increased network efficiency or global integration may be a general developmental phenomenon that can be observed in both intrinsic and extrinsic functional networks. Notably, the hypothesized imbalanced development between the reward system and cognitive control system during adolescence (Casey, 2015; Shulman et al., 2016) could be reflected in the lower functional connectivity and topological efficiency of the brain's reward network that we observed at T1. It is possible that the temporal changes that we report in brain response and functional networks are attributed to the synaptic pruning and myelination during development (Spear, 2013).

There were no significant changes in the network clustering coefficient from T1 to T2, suggesting local networks that were involved in the processing of reward had not dramatically changed from adolescence to young adulthood. These findings may reflect that the key architectures recruited in reward anticipation did not change from adolescence to young adulthood, a finding supported by the supplementary analysis showing that regions such as VS, caudate, thalamus, dorsal anterior cingulate and insula were reliably activated by reward anticipation at both T1 and T2. The task-modulated functional network, in which high-level task demands are accommodated by context-specific modulations, is not equivalent to the intrinsic functional network (Mennes et al., 2013). Therefore, our study provides a complementary characterization of brain development to previous resting-state fMRI studies (Ernst et al., 2015).

One motivation for focusing on reward network changes during this developmental period is that it may yield insights into biological risk factors or vulnerability for substance use. We found increased alcohol use at T2 affected the trajectories of functional connectivity between right VS and left MTG. There is some evidence that the grey matter volume of MTG is related to preferences for smaller immediate rewards over larger delayed rewards (Owens et al., 2017). Functions in this region during reward anticipation have previously been associated with substance use (Jollans et al., 2016; Nestor et al., 2020), making this region a promising target for future studies on substance use. For instance, substance addicted individuals with extended abstinence showed less response in temporal and visual regions during reward anticipation compared with controls (Nestor et al., 2020). Furthermore, a previous study showed that connectivity between VS with MTG during reward anticipation was negatively associated with smoking frequency in adolescents (Jollans et al., 2016).

Analysis with the task-modulated network showed that developmental trajectories in the network characteristic shortest path length from T1 to T2 differed in HA and LA groups. The developmental change for both LA and HA groups was a decrease in characteristic shortest path length from T1 to T2. These results may imply that relatively high alcohol use by T2 may disrupt the normal development of network integration during reward anticipation. It is worth noting that disruption in network efficiency has been reported in addiction populations during tasks and rest (Morris et al., 2018; Wang et al., 2018; Nestor et al., 2020). For instance, a previous study found that former addicts had elevated characteristic shortest path length during reward anticipation compared with controls (Nestor et al., 2020), suggesting that disrupted trajectories of network efficiency in response to reward could constitute vulnerability factors for future addiction.

Notably, no significant alcohol effects on trajectories of brain response were found, suggesting connectivity-based measures could be more sensitive measures of the subtle brain correlates of adolescent alcohol use. It has been argued that fMRI tasks are optimal for eliciting robust group-level, task-specific response, to the detriment of investigating between-subject variance in activation (Hedge et al., 2018), leading to reduced sensitivity in detecting subtle effects. It is possible that functional connectivity and global network measures which characterize the relationships between brain regions and properties of whole-brain networks are more sensitive indices of both neurodevelopmental trajectories and alcohol-associated alterations to those trajectories.

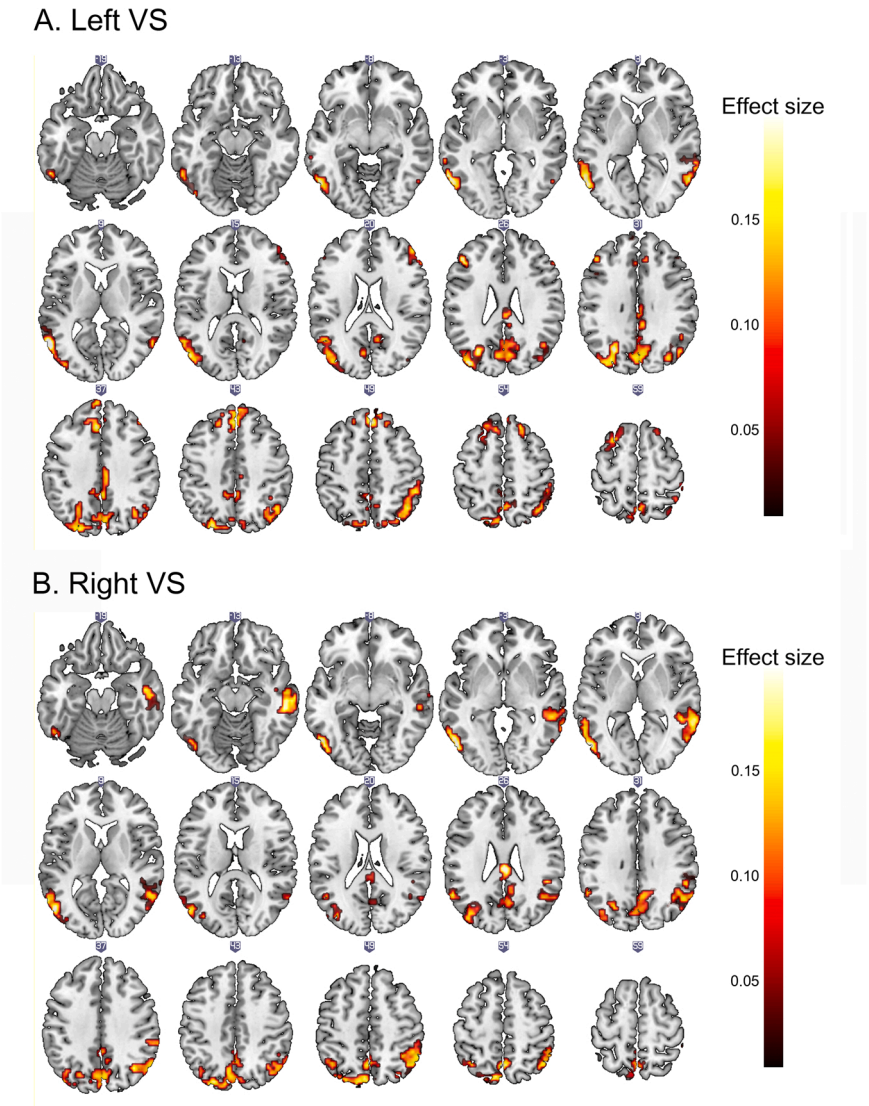

Fig. 4. Regions showing significantly increased functional connectivity with left (A) and right (B) VS during reward anticipation at T2 as compared to T1. The colorbar denotes the effect size.

A few limitations need to be borne in mind when interpreting the results. Due to ethical concerns, participants were given candies at T1. Different reward type between T1 and T2 could be a potential confounding factor. Although equating rewards across large developmental periods is a significant challenge, we note that the behavioural measures (i.e., faster responding for large rewards compared to no rewards) indicated that participants were motivated by the rewards available at both T1 and T2 regardless of how the points were exchanged at the end of the experiment. Another limitation is that the points-to-reward ratio was explicit at T1 (5 points = 1 candy) but was uncertain at T2. However, we suspect that the added uncertainty element at T2 was unlikely to be consequential. The cross-sectional analysis using a probabilistic mapping approach indicated that the key regions involved in reward anticipation largely overlapped between T1 and T2. If the added uncertainty element is consequential, we might predict the recruitment of additional regions that encode uncertainty (e.g., OFC/mPFC). A large number of studies have shown that uncertainty signals are encoded by OFC (Hsu et al., 2005; Knutson et al., 2005; Schultz et al., 2008; Abler et al., 2009). For example, a previous study used a variant of the standard MID task where probabilities (i.e., level of uncertainty) and magnitude of the reward were signaled by different types of cues. This study reported that the VS response was associated with anticipated gain magnitude while the anticipated gain probability was associated with brain response in the mesial prefrontal cortex (Knutson et al., 2005). However, in the present study we found neither a robust response in OFC/mPFC during reward anticipation at T2 nor were there significant differences in brain response in OFC/mPFC between T1 and T2. This may suggest that the added uncertainty element was not explicitly processed or attended to during task performance, due perhaps to the relatively short interval for cue display and reward anticipation preventing participants from a deliberation on the probability of winning the reward. Furthermore, it may be important to note that the uncertainty in the present task may be different in important ways to the uncertainty that is typically researched. Typically, experimental manipulations of uncertainty add a probabilistic element to whether or not a successful response will be rewarded. In contrast, in the T2 task, participants knew that all successful responses would be rewarded and there was no uncertainty that a successful response would yield points won – what was unknown was the value of the points. Moreover, multiple factors such as novelty seeking, family history of drug abuse, genetic variance have been shown related to lower VS response during reward anticipation in previous studies (Büchel et al., 2017; Maričić et al., 2020; Tschorn et al., 2021), which need to be considered in future studies.

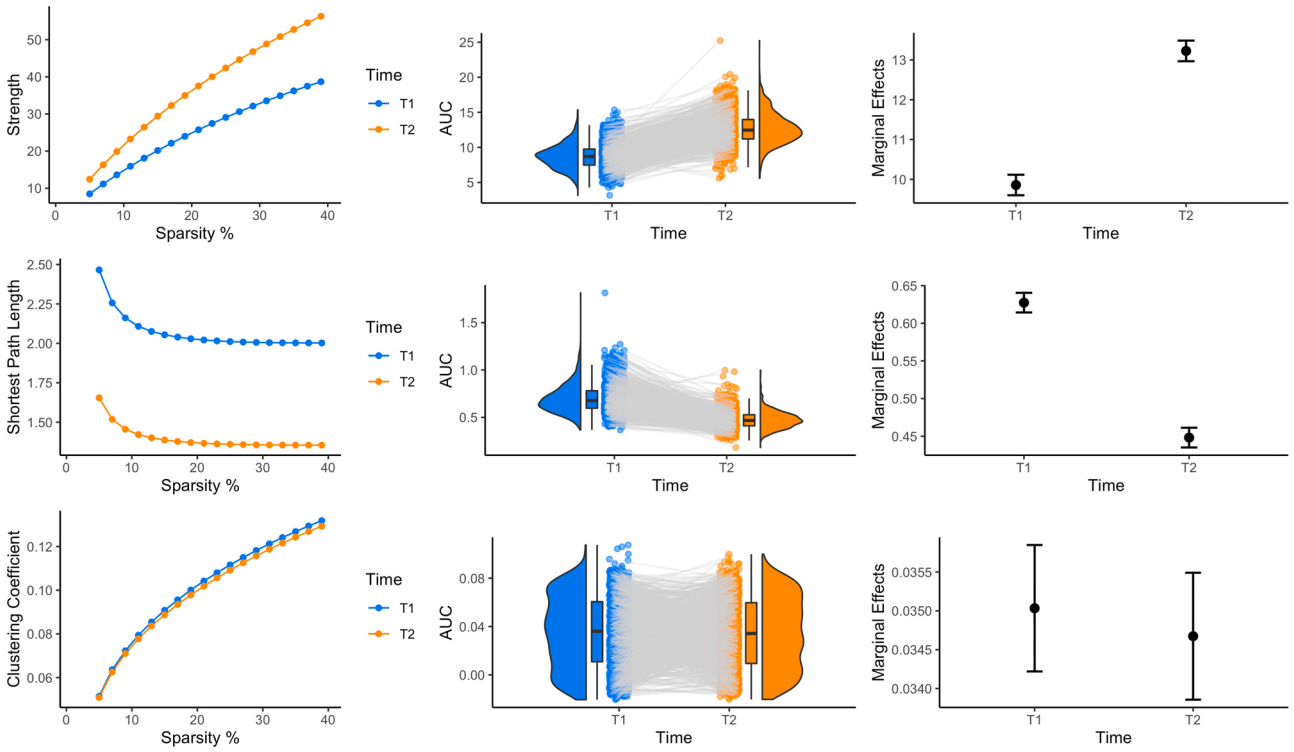

Fig. 5. Network properties at T1 and T2. The plots in the left column show the mean values of network measures for T1 (blue) and T2 (orange) separately across different sparsity thresholds. The plots in the middle columns show the area under the curve of the measures. Each dot represents one participant and participants presented in both T1 and T2 are connected by lines. To alleviate overplotting, a small random noise is added to the dots. The plots in the right columns show the marginal effects of time (T1 vs. T2) calculated using LME models.

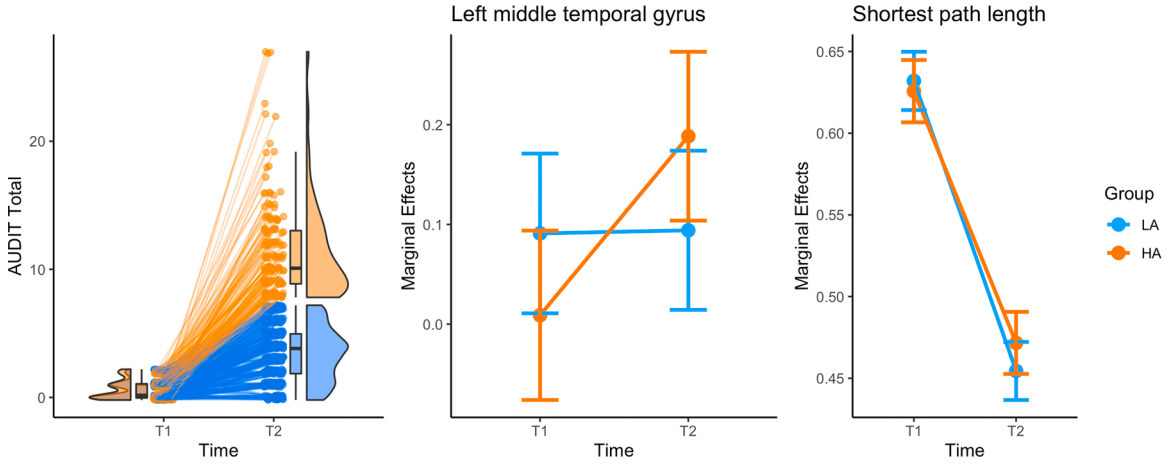

Fig. 6. Left: scatter plot of the AUDIT total scores at T1 and T2. Participants who had a low AUDIT score (≤2) at T1 but a high AUDIT score (≥8) at T2 were designated as the high alcohol use group (HA; orange). Those who had a low AUDIT score at both T1 (≤2) and T2 (≤7) were designated as the low alcohol use group (LA; blue). Each dot represents one participant with their T1 and T2 data connected by lines. Middle: The interaction results between time (T1 vs. T2) and alcohol group (LA vs. HA) for the functional connectivity between left middle temporal gyrus and right VS. To visualize this effect, functional connectivity within a spherical ROI with a 5-mm radius centered at the MNI coordinate of the left middle temporal gyrus was extracted and compared using the LME model. Right: The interaction results for the characteristic shortest path length.

5. Conclusion

Five years of development from early adolescence to young adulthood was characterized by reduced reward-related response in subcortical areas (e.g., VS) and increased response in cortical areas (e.g., IFG, MFG). Mirroring these regional changes, the functional connectivity with the VS increased and the brain network involved in reward anticipation also became more topologically efficient. Notably, this developmental pattern was altered in those who increased their drinking during these years. Collectively, these results demonstrate the utility of the MID task as a probe of typical brain response and network properties during development and of differences in these features related to adolescent drinking, a reward-related behaviour associated with heightened risk for future negative health outcomes.

Declaration of Competing Interest

The authors declare the following financial interests/personal

relationships which may be considered as potential competing interests: Dr Banaschewski served in an advisory or consultancy role for ADHS digital, Infectopharm, Lundbeck, Medice, Neurim Pharmaceuticals, Oberberg GmbH, Roche, and Takeda. He received conference support or speaker's fee by Medice and Takeda. He received royalities from Hogrefe, Kohlhammer, CIP Medien, Oxford University Press; the present work is unrelated to these relationships. Dr Barker has received honoraria from General Electric Healthcare for teaching on scanner programming courses. Dr Poustka served in an advisory or consultancy role for Roche and Viforpharm and received speaker's fee by Shire. She received royalties from Hogrefe, Kohlhammer and Schattauer. The present work is unrelated to the above grants and relationships. The other authors report no biomedical financial interests or potential conflicts of interest.

Data Availability

The data utilized in the present study have not been made publicly available. Further information regarding data availability, please visit https://imagen-europe.com/.

Acknowledgments

This work received support from the following sources: the National Institute on Drug Abuse (NIDA) grant R01DA047119; the European Union-funded FP6 Integrated Project IMAGEN (Reinforcement-related behaviour in normal brain function and psychopathology) (LSHM-CT-2007-037286), the Horizon 2020 funded ERC Advanced Grant 'STRATIFY' (Brain network based stratification of reinforcement-related disorders) (695313), Human Brain Project (HBP SGA 2, 785907, and HBP SGA 3, 945539), the Medical Research Council Grant 'c-VEDA' (Consortium on Vulnerability to Externalizing Disorders and Addictions) (MR/N000390/1), the National Institute of Health (NIH) (R01DA049238, A decentralized macro and micro gene-by-environment interaction analysis of substance use behavior and its brain biomarkers; and R01MH085772, Axon, Testosterone and Mental Health during Adolescence), the National Institute for Health Research (NIHR) Biomedical Research Centre at South London and Maudsley NHS Foundation Trust and King's College London, the Bundesministeriumfür Bildung und Forschung (BMBF grants 01GS08152; 01EV0711; Forschungsnetz AERIAL 01EE1406A, 01EE1406B; Forschungsnetz IMAC-Mind 01GL1745B), the Deutsche Forschungsgemeinschaft (DFG grants SM 80/7-2, SFB 940, TRR 265, NE 1383/14-1), the Medical Research Foundation and Medical Research Council (grants MR/R00465X/1 and MR/S020306/1), the National Institutes of Health (NIH) funded ENIGMA (grants 5U54EB020403-05 and 1R56AG058854-01). Further support was provided by grants from: - the ANR (ANR-12-SAMA-0004, AAPG2019 - GeBra), the Eranet Neuron (AF12-NEUR0008-01 - WM2NA; and ANR-18-NEUR00002-01 - ADORe), the Fondation de France (00081242), the Fondation pour la Recherche Médicale (DPA20140629802), the Mission Interministérielle de Lutte-contre-les-Drogues-et-les-Conduites-Addictives (MILDECA), the Assistance-Publique-Hôpitaux-de-Paris and INSERM (interface grant), Paris Sud University IDEX 2012, the Fondation de l'Avenir (grant AP-RM-17-013), the Fédération pour la Recherche sur le Cerveau; the National Institutes of Health, Science Foundation Ireland (16/ERCD/3797), U.S.A. (Axon, Testosterone and Mental Health during Adolescence; RO1 MH085772-01A1), and by NIH Consortium grant U54 EB020403, supported by a cross-NIH alliance that funds Big Data to Knowledge Centres of Excellence, the National Institute for Health Research (NIHR) Biomedical Research Centre (BRC) at South London and Maudsley NHS Foundation Trust (SLaM) and King's College London (KCL). ImagenPathways "Understanding the Interplay between Cultural, Biological and Subjective Factors in Drug Use Pathways" is a collaborative project supported by the European Research Area Network on Illicit Drugs (ERANID). This paper is based on independent research commissioned and funded in England by the National Institute for Health Research (NIHR) Policy Research Programme (project ref. PR-ST-0416-10001). The views expressed in this article are those of the authors and not necessarily those of the national funding agencies or ERANID.

Appendix A. Supporting information

Supplementary data associated with this article can be found in the online version at doi:10.1016/j.dcn.2021.101042.

References

Abler, B., Herrnberger, B., Grön, G., Spitzer, M., 2009. From uncertainty to reward: BOLD characteristics differentiate signaling pathways. BMC Neurosci. 10, 1–12.
Anderson, B.A., 2016. The attention habit: how reward learning shapes attentional selection. Ann. N. Y. Acad. Sci. 1369, 24–39.
Behzadi, Y., Restom, K., Liau, J., Liu, T.T., 2007. A component based noise correction method (CompCor) for BOLD and perfusion based fMRI. Neuroimage 37, 90–101.
Bjork, J.M., Smith, A.R., Chen, G., Hommer, D.W., 2010. Adolescents, adults and rewards: comparing motivational neurocircuitry recruitment using fMRI. PLoS One 5, e11440.
Bjork, J.M., Knutson, B., Fong, G.W., Caggiano, D.M., Bennett, S.M., Hommer, D.W., 2004. Incentive-elicited brain activation in adolescents: similarities and differences from young adults. J. Neurosci. 24, 1793–1802.
Boehler, C.N., Hopf, J.-M., Krebs, R.M., Stoppel, C.M., Schoenfeld, M.A., Heinze, H.-J., Noesselt, T., 2011. Task-load-dependent activation of dopaminergic midbrain areas in the absence of reward. J. Neurosci. 31, 4955–4961.
Breckel, T.P., Giessing, C., Thiel, C.M., 2011. Impact of brain networks involved in vigilance on processing irrelevant visual motion. Neuroimage 55, 1754–1762.
Büchel, C., Peters, J., Banaschewski, T., Bokde, A.L., Bromberg, U., Conrod, P.J., Flor, H., Papadopoulos, D., Garavan, H., Gowland, P., 2017. Blunted ventral striatal responses to anticipated rewards foreshadow problematic drug use in novelty-seeking adolescents. Nat. Commun. 8, 1–11.
Cao, Z., Bennett, M., Orr, C., Icke, I., Banaschewski, T., Barker, G.J., Bokde, A.L., Bromberg, U., Büchel, C., Quinlan, E.B., 2019. Mapping adolescent reward anticipation, receipt, and prediction error during the monetary incentive delay task. Hum. Brain Mapp. 40, 262–283.
Casey, B., 2015. Beyond simple models of self-control to circuit-based accounts of adolescent behavior. Ann. Rev. Psychol. 66, 295–319.
Conigrave, K.M., Hall, W.D., Saunders, J.B., 1995. The AUDIT questionnaire: choosing a cut-off score. Addiction 90, 1349–1356.
Corbetta, M., Shulman, G.L., 2002. Control of goal-directed and stimulus-driven attention in the brain. Nat. Rev. Neurosci. 3, 201–215.
Di, X., Biswal, B.B., 2019. Toward task connectomics: examining whole-brain task modulated connectivity in different task domains. Cereb. Cortex 29, 1572–1583.
Dosenbach, N.U., Nardos, B., Cohen, A.L., Fair, D.A., Power, J.D., Church, J.A., Nelson, S. M., Wig, G.S., Vogel, A.C., Lessov-Schlaggar, C.N., 2010. Prediction of individual brain maturity using fMRI. Science 329, 1358–1361.
Ernst, M., Torrisi, S., Balderston, N., Grillon, C., Hale, E.A., 2015. fMRI functional connectivity applied to adolescent neurodevelopment. Ann. Rev. Clin. Psychol. 11, 361–377.
Ernst, M., Nelson, E.E., Jazbec, S., McClure, E.B., Monk, C.S., Leibenluft, E., Blair, J., Pine, D.S., 2005. Amygdala and nucleus accumbens in responses to receipt and omission of gains in adults and adolescents. Neuroimage 25, 1279–1291.
Fair, D.A., Dosenbach, N.U., Church, J.A., Cohen, A.L., Brahmbhatt, S., Miezin, F.M., Barch, D.M., Raichle, M.E., Petersen, S.E., Schlaggar, B.L., 2007. Development of distinct control networks through segregation and integration. Proc. Natl. Acad. Sci. 104, 13507–13512.
Finn, E.S. , 2021. Is it time to put rest to rest? Trends Cogn. Sci. 25, 1021-1032.
Friston, K., Buechel, C., Fink, G., Morris, J., Rolls, E., Dolan, R.J., 1997. Psychophysiological and modulatory interactions in neuroimaging. Neuroimage 6, 218–229.
Galvan, A., Hare, T.A., Parra, C.E., Penn, J., Voss, H., Glover, G., Casey, B., 2006. Earlier development of the accumbens relative to orbitofrontal cortex might underlie risk-taking behavior in adolescents. J. Neurosci. 26, 6885–6892.
Hedge, C., Powell, G., Sumner, P., 2018. The reliability paradox: why robust cognitive tasks do not produce reliable individual differences. Behav. Res. Methods 50, 1166–1186.
Hsu, M., Bhatt, M., Adolphs, R., Tranel, D., Camerer, C.F., 2005. Neural systems responding to degrees of uncertainty in human decision-making. Science 310, 1680–1683.
Jollans, L., Zhipeng, C., Icke, I., Greene, C., Kelly, C., Banaschewski, T., Bokde, A.L., Bromberg, U., Büchel, C., Cattrell, A., 2016. Ventral striatum connectivity during reward anticipation in adolescent smokers. Dev. Neuropsychol. 41, 6–21.
Knight, J.R., Sherritt, L., Harris, S.K., Gates, E.C., Chang, G., 2003. Validity of brief alcohol screening tests among adolescents: a comparison of the AUDIT, POSIT, CAGE, and CRAFFT. Alcohol. Clin. Exp. Res. 27, 67–73.
Knutson, B., Taylor, J., Kaufman, M., Peterson, R., Glover, G., 2005. Distributed neural representation of expected value. J. Neurosci. 25, 4806–4812.
Kuznetsova, A., Brockhoff, P.B., Christensen, R.H., 2017. lmerTest package: tests in linear mixed effects models. J. Stat. Softw. 82, 1–26.

Lorenz, R.C., Gleich, T., Beck, A., Pöhland, L., Raufelder, D., Sommer, W., Rapp, M.A., Kühn, S., Gallinat, J., 2014. Reward anticipation in the adolescent and aging brain. Hum. Brain Mapp. 35, 5153–5165.
Lv, H., Wang, Z., Tong, E., Williams, L.M., Zaharchuk, G., Zeineh, M., Goldstein-Piekarski, A.N., Ball, T.M., Liao, C., Wintermark, M., 2018. Resting-state functional MRI: everything that nonexperts have always wanted to know. Am. J. Neuroradiol. 39, 1390–1399.
Mackey, S., Chaarani, B., Kan, K.-J., Spechler, P.A., Orr, C., Banaschewski, T., Barker, G., Bokde, A.L., Bromberg, U., Büchel, C., 2017. Brain regions related to impulsivity mediate the effects of early adversity on antisocial behavior. Biol. Psychiatry 82, 275–282.
Maričić, L.M., Walter, H., Rosenthal, A., Ripke, S., Quinlan, E.B., Banaschewski, T., Barker, G.J., Bokde, A.L., Bromberg, U., Büchel, C., 2020. The IMAGEN study: a decade of imaging genetics in adolescents. Mol. Psychiatry 25, 2648–2671.
Mennes, M., Kelly, C., Colcombe, S., Castellanos, F.X., Milham, M.P., 2013. The extrinsic and intrinsic functional architectures of the human brain are not equivalent. Cereb. Cortex 23, 223–229.
Morris, L.S., Baek, K., Tait, R., Elliott, R., Ersche, K.D., Flechais, R., McGonigle, J., Murphy, A., Nestor, L.J., Orban, C., 2018. Naltrexone ameliorates functional network abnormalities in alcohol-dependent individuals. Addic. Biol. 23, 425–436.
Nestor, L.J., Suckling, J., Ersche, K.D., Murphy, A., McGonigle, J., Orban, C., Paterson, L. M., Reed, L., Taylor, E., Flechais, R., 2020. Disturbances across whole brain networks during reward anticipation in an abstinent addiction population. NeuroImage Clin. 27, 102297.
O'Connor, E.A., Perdue, L.A., Senger, C.A., Rushkin, M., Patnode, C.D., Bean, S.I., Jonas, D.E., 2018. Screening and behavioral counseling interventions to reduce unhealthy alcohol use in adolescents and adults: updated evidence report and systematic review for the US Preventive Services Task Force. JAMA 320, 1910–1928.
Oldham, S., Murawski, C., Fornito, A., Youssef, G., Yücel, M., Lorenzetti, V., 2018. The anticipation and outcome phases of reward and loss processing: a neuroimaging meta-analysis of the monetary incentive delay task. Hum. Brain Mapp. 39, 3398–3418.
Owens, M.M., Gray, J.C., Amlung, M.T., Oshri, A., Sweet, L.H., MacKillop, J., 2017. Neuroanatomical foundations of delayed reward discounting decision making. NeuroImage 161, 261–270.
Petersen, A.C., Crockett, L., Richards, M., Boxer, A., 1988. A self-report measure of pubertal status: Reliability, validity, and initial norms. J. Youth Adolesc. 17, 117–133.
Power, J.D., Barnes, K.A., Snyder, A.Z., Schlaggar, B.L., Petersen, S.E., 2012. Spurious but systematic correlations in functional connectivity MRI networks arise from subject motion. Neuroimage 59, 2142–2154.
Reinert, D.F., Allen, J.P., 2002. The alcohol use disorders identification test (AUDIT): a review of recent research. Alcohol. Clin. Exp. Res. 26, 272–279.
Richards, J.M., Plate, R.C., Ernst, M., 2013. A systematic review of fMRI reward paradigms used in studies of adolescents vs. adults: the impact of task design and implications for understanding neurodevelopment. Neurosci. Biobehav. Rev. 37, 976–991.
Rorden, C., Brett, M., 2000. Stereotaxic display of brain lesions. Behav. Neurol. 12, 191–200.
Schneider, S., Peters, J., Bromberg, U., Brassen, S., Miedl, S.F., Banaschewski, T., Büchel, C., 2012b. Risk taking and the adolescent reward system: A potential common link to substance abuse. The American Journal of Psychiatry 169, 39–46.
Schneider, S., Brassen, S., Bromberg, U., Banaschewski, T., Conrod, P., Flor, H., Büchel, C., 2012a. Maternal interpersonal affiliation is associated with adolescents' brain structure and reward processing. Translational Psychiatry 2, e182.
Sarter, M., Gehring, W.J., Kozak, R., 2006. More attention must be paid: the neurobiology of attentional effort. Brain Res. Rev. 51, 145–160.
Schultz, W., Preuschoff, K., Camerer, C., Hsu, M., Fiorillo, C.D., Tobler, P.N., Bossaerts, P., 2008. Explicit neural signals reflecting reward uncertainty. Philos. Trans. R. Soc. B Biol. Sci. 363, 3801–3811.
Schumann, G., Loth, E., Banaschewski, T., Barbot, A., Barker, G., Büchel, C., Conrod, P., Dalley, J., Flor, H., Gallinat, J., 2010. The IMAGEN study: reinforcement-related behaviour in normal brain function and psychopathology. Mol. Psychiatry 15, 1128–1139.
Shulman, E.P., Smith, A.R., Silva, K., Icenogle, G., Duell, N., Chein, J., Steinberg, L., 2016. The dual systems model: review, reappraisal, and reaffirmation. Dev. Cognit. Neurosci. 17, 103–117.
Smith, S.M., Nichols, T.E., 2009. Threshold-free cluster enhancement: addressing problems of smoothing, threshold dependence and localisation in cluster inference. Neuroimage 44, 83–98.
Spear, L.P., 2013. Adolescent neurodevelopment. J. Adolesc. Health 52, S7–S13.
Stevens, M.C., 2016. The contributions of resting state and task-based functional connectivity studies to our understanding of adolescent brain network maturation. Neurosci. Biobehav. Rev. 70, 13–32.
Tschorn, M., Lorenz, R.C., O'Reilly, P.F., Reichenberg, A., Banaschewski, T., Bokde, A.L., Quinlan, E.B., Desrivières, S., Flor, H., Grigis, A., 2021. Differential predictors for alcohol use in adolescents as a function of familial risk. Trans. Psychiatry 11, 1–11.
Vaidya, J.G., Knutson, B., O'Leary, D.S., Block, R.I., Magnotta, V., 2013. Neural sensitivity to absolute and relative anticipated reward in adolescents. PLoS One 8, e58708.
Vassena, E., Silvetti, M., Boehler, C.N., Achten, E., Fias, W., Verguts, T., 2014. Overlapping neural systems represent cognitive effort and reward anticipation. PLoS One 9, e91008.
Wang, J., Zuo, X., Gohel, S., Milham, M.P., Biswal, B.B., He, Y., 2011. Graph theoretical analysis of functional brain networks: test-retest evaluation on short-and long-term resting-state functional MRI data. PLoS One 6, e21976.
Wang, J., Wang, X., Xia, M., Liao, X., Evans, A., He, Y., 2015. GRETNA: a graph theoretical network analysis toolbox for imaging connectomics. Front. Hum. Neurosci. 9, 386.
Wang, Y., Zhao, Y., Nie, H., Liu, C., Chen, J., 2018. Disrupted brain network efficiency and decreased functional connectivity in multi-sensory modality regions in male patients with alcohol use disorder. Front. Hum. Neurosci. 12, 513.
WHO, 2001. AUDIT: The Alcohol use Disorders Identification Test: Guidelines for use in Primary Health Care. World Health Organization.
Yacubian, J., Glascher, J., Schroeder, K., Sommer, T., Braus, D.F., Büchel, C., 2006. Dissociable systems for gain- and loss-related value predictions and errors of prediction in the human brain. The Journal of Neuroscience 26, 9530–9537.